scientific reports

Check for updates

OPEN

Natural genetic variation impacts complement inhibitory activity of PFam54 orthologs of Asian *Borrelia bavariensis*

Luisa Langhoff[1,8], Paul Kapfer[1,8], Florian Röttgerding[1], Gabriele Margos[2], Sabrina Hepner[2], Volker Fingerle[2], Kozue Sato[3], Hiroki Kawabata[3], Yi-Pin Lin[4], Kalvis Brangulis[5,6], Robert E. Rollins[7,9] & Peter Kraiczy[1,9]✉

European and Asian populations of *Borrelia (B.) bavariensis*, a causative agent of Lyme borreliosis, substantially differ in their infection dynamics. This is argued to be a byproduct of the unique demographic history of *B. bavariensis* in relation to colonizing Europe from a highly diverse, ancestral Asian population. Whether genetic factors related to human disease could be unique traits associated with the demographic history of the European population though remains largely unclear. European *B. bavariensis* possesses at least two anti-complement determinants, BGA66 and BGA71 encoding by genes of the PFam54 gene array. In Asian *B. bavariensis* populations, the composition of this gene array is highly diverse. To assess functional integrity of PFam54 orthologs, two Asian *B. bavariensis* isolates, NT24 and JHM1114, were investigated. Despite the substantial observed genetic diversity, the complement-inhibitory and cell-protective function of BGA66 and BGA71 orthologs are largely conserved among European and Asian populations. We also identified two novel PFam54 orthologs of Asian origin, BGA67b and BGA71b, both of which display anti-complement activity on the terminal pathway and confer serum resistance. Taken together, our findings highlight the importance of studying natural variation of proteins potentially involved in immune escape, pathogenesis, and host adaptation.

Keywords Lyme disease, Spirochetes, Borrelia, Immune evasion, Complement, Innate immunity, PFam54 family

Lyme borreliosis (LB) is the most common vector-borne disease in the northern hemisphere caused by spirochetes of the *Borrelia (B.) burgdorferi* sensu lato complex[1,2], and maintained in complex transmission cycles between various tick vectors and reservoir hosts[1]. Almost all LB cases in North America are caused by the species *B. burgdorferi* sensu stricto, hereafter termed *B. burgdorferi*, while *B. afzelii*, *B. garinii*, *B. spielmanii* and *B. bavariensis* are causative agents of LB across Eurasia[1–5].

LB is considered a multi-systemic disorder in which the skin, musculoskeletal or central nervous system can be affected. Improper treatment may progress to more prominent clinical manifestations including chronic skin lesions, persistent arthritis or severe neurological complications[6,7]. A general organotropism has frequently been discussed for some species[5,8,9] but is not apparent for *B. bavariensis*. While European *B. bavariensis* isolates display a marked tropism for neurological tissues, Asian strains apparently do not[5,10]. Unlike other species, *B. bavariensis* displays a unique demographic history hypothesized to be in association with invading the European tick vector, *Ixodes ricinus*[4,11,12]. This vector switch led to a selective bottleneck resulting in an almost

[1]Institute of Medical Microbiology and Infection Control, Goethe University Frankfurt, University Hospital of Frankfurt, Frankfurt, Germany. [2]National Reference Center for Borrelia, Bavarian Health and Food Safety Authority, Oberschleissheim, Germany. [3]Department of Bacteriology-I, National Institute of Infectious Diseases, Tokyo, Japan. [4]Department of Infectious Disease & Global Health, Cumming School of Veterinary Medicine, Tufts University, North Grafton, USA. [5]Latvian Biomedical Research and Study Centre, Riga, Latvia. [6]Department of Human Physiology and Biochemistry, Riga Stradins University, Riga, Latvia. [7]Institute of Avian Research "Vogelwarte Helgoland", Wilhelmshaven, Germany. [8]Luisa Langhoff and Paul Kapfer contributed equally to this work. [9]These authors jointly supervised this work: Robert E. Rollins, Peter Kraiczy. ✉email: Kraiczy@em.uni-frankfurt.de

clonal distribution of European *B. bavariensis*[4,11,13]. A hypothesized byproduct of this selective sweep, is the emergence of genetic variants related to this vector shift, which additionally increase the likelihood of isolates causing human LB[4]. Previous work on other *Borrelia* species (i.e., *B burgdorferi*, *B. afzelii*) have shown that little variation can greatly influence protein functionality for infecting the host[14–18]. As substantial genetic variation exists between Asian and European *B. bavariensis* populations[12,13,19], we hypothesize that genetic variation could influence known mechanisms of human infection (e.g., interactions with the hosts immune system). Even so, no functional study exists to date testing this hypothesis.

To establish an infection, *Borrelia* must evade host immune responses including complement, an important pillar of human innate immunity. The complement system consists of three canonical pathways, the classical (CP), the lectin (LP), and the alternative pathway (AP)[20]. To control excessive complement activation, host cells are protected by either membrane-bound or fluid-phase regulators[20] leading to the termination of the complement cascade at certain levels[20]. To evade complement, *Borrelia* possess a number of functionally diverse proteins which are encoded by genes distributed on various plasmids[21–23]. Members belonging to the paralogous protein family 54 (PFam54) are known to confer serum resistance by binding complement regulators (e.g., CspA binding complement regulator factor H (FH) and FH-like protein 1 (FHL-1)) or by interacting directly with complement proteins[15,24–27]. The PFam54 genes are predominantly arranged in a gene array located near the 3′end of the linear plasmid (lp) 54 in almost all *Borrelia* genomes studied[28–31] highlighting potential selective pressures for the maintenance of this gene family over time. This array is separated into five Clades (I, II, III, IV, V)[29,31,32], with Clade IV containing the prototypic FH binding protein CspA as well as other proteins interacting with complement members. PFam54 orthologs belonging to all five Clades are present in *B. bavariensis* isolates but the biological function(s) of these proteins has not yet been fully assessed. *Borrelia bavariensis* isolates do not possess an ortholog mirroring the same complement-inhibitory function of CspA, but do contain two distinct PFam54 Clade IV molecules, BGA66 and BGA71, capable of binding complement proteins and inhibiting the terminal pathway (TP)[25]. Both proteins lack FH/FHL-1 binding activity but interact with C7, C8, and C9 to efficiently block TP activation and membrane attack complex formation. Apparently, the direct interaction with the late complement components strongly affects MAC assembly and thereby efficiently terminate TP activation. In contrast, serum-resistant *B. bavariensis* develop alternative strategies to successfully overcome complement-mediated killing already known from serum-resistant *B. burgdorferi*, *B. mayonii*, *B. afzelii*, and *B. spielmanii*, respectively, all of which block complement activation by acquisition of the key complement regulators of the AP, FH and FHL-1. So far, no information is available on the complement inhibitory potential of other Clade IV paralogs of *B. bavariensis* PBi (e.g., BGA67, BGA68).

All functional analyses to date have been performed on the European type strain PBi and it is currently not known if these functions are conserved in Asian *B. bavariensis* isolates which display a high level of genetic variation in comparison to European *B. bavariensis* isolates[12,13,19]. This includes a recent study describing the PFam54 array architecture of various isolates, showing the absence of genes encoding BGA66 and BGA71 in certain Asian isolates (15–20% of sequenced isolates)[32]. As these genes are of importance to protect the European type strain PBi, it brings forward the question if their absence makes certain Asian isolates susceptible to human complement or if other genes unique to Asian isolates could have yet unknown complement-inhibitory function. The same study showed that Asian isolates contain three novel PFam54 orthologs, *bga67b*, *bga68b*, and *bga71b*[32]. Of which only *bga71b* is an ortholog of a *B. bavariensis* gene, representing a recent duplication of *bga71* as found in PBi[32]. If this duplicated gene has similar functionality to BGA71 as observed in PBi, is currently not known. In phylogenetic reconstructions including all PFam54 genes (Clades I-V) from isolates of *B. afzelli*, *B. bavariensis*, and *B. garinii*, it was further shown that both *bga67b* and *bga68b* represent orthologs of *B. garinii* specific genes *zqa68* and *zqa70*, respectively. Of these, only *zqa68* has a known function; encoding a protein capable of specifically binding avian FH and protecting spirochetes from complement mediated-killing by avian serum, but not binding human FH[15]. It is still not clear how much genetic diversity is present among PFam54 genes of the two distinct *B. bavariensis* populations, although higher diversity in Asian isolates, as observed on the whole genome level, is expected[13,19]. With other *Borrelia* studies convincingly showing major impacts of even minimal amounts of genetic variation on protein function[14–18], we hypothesize that variation between Asian and European *B. bavariensis* isolates could also impact protein function in a population specific manner.

To determine this, we aimed to first assess genetic diversity across all PFam54 genes in available *B. bavariensis* genome sequences and then determine if the molecular mechanism of complement inhibition is only found in European *B. bavariensis* isolates or shared between the populations. For this we selected two Japanese *B. bavariensis* isolates (NT24, JHM1114) to test if PFam54 members with known function (BGA66, BGA71) in PBi retain similar functionality in Asian isolates and to further determine if novel Asian PFam54 orthologs display complement-inhibitory function not found in European *B. bavariensis* isolates. The two isolates were chosen to represent the variation within the Asian *B. bavariensis* population, with NT24 having all the same PFam54 orthologs as PBi (including *bga66* and *bga71*) and containing the novel, Asian-specific ortholog *bga68b*[32]. JHM1114 lacks *bga66* and contains all novel, Asian-specific PFam54 orthologs (*bga67b*, *bga68b*, *bga71b*)[32] making it highly dissimilar to PBi and therefore having the potential to capture functional differences due to this. Both isolates further represent common, Asian-specific PFam54 architecture types and arise from low diversity clades containing multiple isolates in the reconstructed phylogenies suggesting their inclusion could be representative for these clades[13,32]. In sum, we aim to gain deeper insight into the role of the highly variable PFam54 protein family in immune evasion and determine if the biological functions are stable across demographically distinct *B. bavariensis* populations.

Materials and methods

Bioinformatic analyses of PFam54 genes

The PFam54 gene arrays and full lp54 sequences for all *B. bavariensis* isolates included in this study were taken from a recently published dataset[13,32]. Full information on isolates used in this study can be found in **Supplementary Table S1**. Assembled lp54 sequences (https://data.mendeley.com/datasets/xy8wt4ty8f/1) were uploaded and annotated using the RAST annotation server[33,34]. Orthologous sequences were determined by using the CRBHits package as implemented in R v.3.5.2[35,36] as described in[13]. Briefly, all coding sequences for each lp54 were compared pairwise to all other lp54 sequences using the *crb2rbh* function. This information was fed into the integrated DAGchainer[37] command to create links between orthologous genes. Orthologous groups were then determined using the "cluster_infomap" command as implemented from the *igraph* R-package[38] on a matrix of gene names and DAGchainer links. FASTA files for all orthologous groups were generated and aligned using MUSCLE v3.8.425[39,40]. Genes found in at least 80% of the isolates (38/47 isolates) were kept and any genes showing overlap with the PFam54 gene array were removed for calculating lp54-specific background distributions. This led to 50 orthologous, lp54-located genes present in at least 80% of the *B. bavariensis* isolates, which were used to estimate background distributions for population genetic statistics. For all lp54-located genes and the PFam54 orthologs separately, nucleotide diversity (π)[41] was estimated in the package *pegas*[42], while ratios of synonymous to non-synonymous mutations (*dN/dS*) were estimated in the package *seqinr*[43,44]. All analyses were run in R v.3.5.2[35]. Nucleotide diversity for all genes was calculated separately for each population (Asian, i.e., hypothesized to be vectored by *I. persulcatus*; European, i.e., vectored by *I. ricinus*[4,45,46], while ratios of synonymous to non-synonymous mutations were estimated across all sequences of a given gene for both populations due to very low diversity in European isolates posing challenges to calculate European specific *dN/dS* ratios. Additionally, as the demographic event occurred on the entire European *B. bavariensis* population, potential divergence is expected to have occurred between not within a single population. PFam54 ortholog values for π and *dN/dS* were considered significantly different to the background distributions if their estimated value was greater than $\mu \pm 2 \times SD$ based on all lp54 genes (excluding the PFam54) where μ is the mean value and SD is the standard deviation cross all values. This method was used (1) as diversity can be highly specific to genomic compartments so a lp54-specific distribution allows for comparison along the same plasmid and (2) was based on the principle that significance at a scale of $p = 0.05$ within Gaussian distributions containing 95% of observations within the interval $\mu \pm 2\sigma$ making it more probable to be true instead of due to stochastic chance.

To visualize differences between the protein sequences encoded by genes present in *B. bavariensis* PBi, NT24, and JHM1114 (isolate choice described below), we first aligned the sequences using MUSCLE as implemented in AliView[47]. Differences in the sequences were visualized in ESPript 3.0[48] using the online server (ESPript - https://espript.ibcp.fr). Amino acid similarities were determined in ESPript 3.0 using the setting %Equivalent, which compares proposed physio-chemical properties, with a global score set to 0.7.

Bacterial strains and culture conditions

Low-passage (< 20) *B. bavariensis* isolate NT24 (tick isolate, Japan), *B. bavariensis* isolate JAASAAM1114 (abbreviated to JHM1114 in this manuscript, tick isolate, Japan), and *B. bavariensis* PBi (human isolate, CSF, Germany) as well as the high-passaged (> 40) *B. garinii* strain G1 (human isolate, CSF, Germany) were cultured until mid-exponential phase (5×10^7 cells per ml) at 33 °C in Barbour-Stoenner-Kelly (BSK-H) medium (Bio&SELL GmbH, Feucht, Germany) supplemented with 7.4% rabbit serum (Sigma Aldrich, St. Louis, MO, USA). All gain-of-function *Borrelia* strains were cultured in BSK-H complete medium supplemented with 100 µg/ml streptomycin. *Escherichia coli* strains producing proteins of *Borrelia* origin were grown at 37 °C in yeast tryptone broth supplemented with the appropriate antibiotics (ampicillin or streptomycin) as previously described in[49].

Human sera, monoclonal and polyclonal antibodies, and human serum proteins

Nonimmune human serum (NHS) collected from at least 10 healthy volunteers was tested for the presence of anti-*Borrelia* IgM and IgG antibodies as previously described[50]. Only sera proven to be negative were used to form the serum pool. Complement activity of the pool was tested by a commercial functional complement assay (SVAR Life Science, Malmö, Sweden). Complement components C5-6, C7, C8, and C9 were purchased from Complement Technology (Tyler, TX, USA), vitronectin was from Merck (Darmstadt, Germany) and the neoepitope-specific anti-C5b-9 antibody were from Quidel (San Diego, CA, USA).

Generation of vectors and purification of His-tagged proteins

The generation of vectors producing amino-terminally hexahistidine (His_6)-tagged proteins BGA66, BGA67, BGA68, and BGA71 from European *B. bavariensis* PBi, CspA (BBA68) and $BBK32_{205}$ from *B. burgdorferi* B31, and CipA from *Acinetobacter baumannii*, respectively, are described elsewhere[25,50–52].

To produce recombinant proteins, the BGA66-, BGA67-, BGA68-, BGA68b-, and BGA71-encoding genes from *B. bavariensis* NT24, and the BGA67b- and BGA71b-encoding genes from *B. bavariensis* JHM1114 were amplified by PCR using primers listed in **Supplementary Table S2**. Following PCR amplification and digestion, the DNA fragments were cloned into the expression vector pQE-30 Xa (QIAGEN, Hilden, Germany). The resulting plasmids were then used to transform *E. coli* BL21 Star (DE3) cells (Thermo Fisher Scientific, Waltham, MA USA) and plasmids from selected clones were then sequenced to ensure that no mutations were incorporated during PCR and subsequent cloning procedure. The production and purification of recombinant proteins have been described previously[53].

To generate different shuttle vectors, genomic DNA isolated from Asian *B. bavariensis* NT24 and JHM1114 as well as European *B. bavariensis* PBi was used as template for PCR amplification with primers listed in **Supplementary Table S2.** DNA fragments encompassing the respective BGA encoding gene and the adjacent

non-coding regions of each gene were then amplified. Following digestion, the purified DNA fragments were subsequently cloned into the shuttle vector pKFSS1[54]. Plasmids were prepared from presumptive *E. coli* clones with the Monarch Plasmid Kit (New England Biolabs, Frankfurt, Germany) and the inserted DNA was sequenced (Eurofins Genomics, Ebersberg, Germany) to ensure that no mutations were introduced during PCR amplification.

SDS-PAGE and Western blot analysis

His_6-tagged proteins were purified by affinity chromatography from crude *E. coli* cell lysates, separated by 10% Tris/tricine SDS-PAGE, and transferred to nitrocellulose membranes as described previously[53]. Briefly, the nitrocellulose membranes were blocked with 5% nonfat dry milk in TBS containing 0.1% Tween 20 (TBS-T). After three wash steps with TBS-T, membranes were incubated with a mixture of anti-His antibodies (1:3,000) followed by horseradish peroxidase-conjugated anti-mouse immunoglobulins (1:1,000). Protein-antigen complexes were then detected by tetramethylbenzidine as substrate as described previously[55]. Images of the gels and nitrocellulose membranes were processed by using a GS-900 calibrated densitometer (Bio-Rad) and the ImageLab software version 6.1 (Bio-Rad).

Complement inactivation assays

To assess the inhibitory capacity of purified, His_6-tagged proteins on the classical (CP) and alternative pathway (AP), an ELISA-based immunoassay was conducted as described recently[56]. In brief, for CP activation, microtiter plates were coated with human IgM (30 ng/ml) (Merck, Darmstadt, Germany) and for AP activation, plates were immobilized with LPS (100 ng/ml) (Hycult Biotech, Beutelsbach, Germany) at 4 °C overnight. Microtiter plates were washed three times with TBS containing 0.05% (v/v) Triton X-100 (TBS-T) and then blocked with PBS-T for 2 h at RT. In parallel, NHS (1% for the CP and 15% for the AP) was pre-incubated with purified His_6-tagged proteins (4 µM each) for 15 min at RT before being added to the wells. The microtiter plates were then washed again three times with TBS-T. To detect the membrane attack complex, a monoclonal neoepitope-specific anti-C5b-9 antibody (1:500) (QuidelOrtho, San Diego, CA, USA) was added. Following incubation for 1 h at RT, wells were washed thoroughly with TBS-T. After incubation with HRP-conjugated anti-mouse immunoglobulins (1:1000) for 1 h at RT, reactions were developed using TMB.

In order to examine the inhibitory potential of purified His_6-tagged proteins on the terminal pathway, a hemolytic assay was conducted as previously described[50]. Initially, sheep erythrocytes (1.5×10^8 cells) were first sensitized by incubating the cells with the C5b-6 complex (1.5 µg/ml) for 10 min at RT. Reaction mixtures containing C7 (2 µg/ml), C8 (0.4 µg/ml), C9 (2 µg/ml), and the respective His_6-tagged proteins (0.5, 1, and 2 µM) in Mg-EGTA buffer were incubated for 5 min at RT. Increasing concentrations of purified His-tagged proteins were tested in parallel in this assay to overcome the short half-life of sheep erythrocytes and to generate comparable datasets. Control reaction mixtures containing BSA or without His_6-tagged proteins were also assayed. The pre-incubated reaction mixtures were the added to the C5b-6 coated sheep erythrocytes and incubated for 30 min at 37 °C. After centrifugation of the erythrocytes, supernatants were then transferred to microtiter plates and hemolysis was determined by measuring the absorbance at 414 nm.

C9 polymerization assay

To assess the inhibitory capacity of borrelial proteins on C9 polymerization, reaction mixtures containing either C9 (3 µg) alone (control) or C9 and the BGA orthologs or control proteins (5–10 µg each) were incubated for 40 min at 37 °C as previously described[24,25]. Fifty microliters of $ZnCl_2$ were then added to the reactions to induce auto-polymerization of C9. As additional controls, all reactions were assayed without $ZnCl_2$. Following incubation for 2 h at 37 °C, reaction mixtures were loaded on 7.5% Laemmli-SDS gels and C9 monomers and polymers were then visualized by silver staining.

Generation of serum-sensitive *B. garinii* strains ectopically producing BGA orthologs

To generate gain-of-function strains carrying shuttle vectors for producing of BGA orthologs, the high-passage and non-infectious *Borrelia garinii* strain G1 was selected as described previously[25]. Spirochetes grown at mid-exponential phase (5×10^7 to 1×10^8 cells/ml) in BSK-H medium were centrifuged and resuspended in electroporation buffer to prepare electrocompetent cells as previously described. In brief, electrocompetent *B. garinii* G1 cells (50 µl each) were electroporated at 12.5 kV/cm with 20 µg of the respective shuttle vector. Thereafter, spirochetes were immediatley transferred into 10 ml of antibiotic-free BSK-H medium and incubated for 18 h at 33 °C. For selection, each culture were diluted in 90 ml BSK-H medium containing streptomycin (25 µg/ml) and 200 µl aliquots were then seeded into 96-well cell culture plates (Corning Costar). Microtiter plates were sealed and incubated at 33 °C until a color change was detectable. Individual clones were collected and expanded in 1 ml of fresh BSK-H medium without antibiotic selection for 7 days, and then transferred into 10 ml of fresh BSK-H medium containing streptomycin (50 µg/ml). Each clone selected was characterized by amplifying the BGA orthologous genes using primers M31 For and M31 Rev (**Supplementary Table S1**) as described[57].

Serum bactericidal assay

A serum bactericidal assay was conducted to analyzed the susceptibility of spirochetes (WT and gain-of-function strains) to human complement as described previously[49]. In brief, *Borrelia* cells grown at mid-logarithmic phase were centrifuged for 10 min at RT and re-suspended in 500 µl fresh BSK-H medium. After counting, 1×10^7 of highly viable spirochetes in 50 µl were treated with either 50 µl of NHS or 50 µl heat-inactivated NHS and incubated at 37 °C with gentle agitation. After 2, 4, and 6 h, the percentage of motile cells were assessed using dark field microscopy by counting nine microscopy fields for each time point per strain. Each test was

independently performed at least three times. It should be noted that motility does not necessarily equate to membrane integrity or long-term survival, and thus represents an indirect measure of bactericidal activity.

AlphaFold structure predictions

AlphaFold v2.0[58] was used to predict the 3D structure for Clade IV orthologs from *B. bavariensis* NT24, JHM1114 and European type strain PBi. Predictions were performed with default parameters as described on the AlphaFold GitHub repository, using an AMD Ryzen Threadripper 2990 WX 32-Core system with 128 GB RAM and four NVIDIA GeForce RTX 2080 GPUs. Databases were downloaded on March 25, 2024. For further analysis, the predicted structure with the highest confidence (based on pLDDT scores) was used.

Statistical analysis

The data collected in this study represent means from at least three independent experiments, and error bars indicate standard deviation (SD). To determine statistical significance, one-way ANOVA analysis with Bonferroni's multiple comparison post-hoc test with a 95% confidence interval was conducted by using GraphPad Prism version 7. Results were deemed statistically significant for the following p values: n.s., not significant, *, $P \leq 0.05$, **, $P \leq 0.01$ ***, $P \leq 0.001$, and ****, $P \leq 0.0001$.

Results

Diversity of PFam54 gene family among Asian *B. bavariensis* isolates

Differences in evolutionary history, as observed for the European and Asian *B. bavariensis* populations[12,13,19], can leave signatures of adaptation which can be quantified using population genetic statistics[59]. As the two populations of *B. bavariensis* appear to differ in neurotropism[5,10], which could reflect a difference in human pathogenicity, we aimed to quantify genetic variation along genes belonging to the PFam54 encoding proteins (BGA66, BGA71) known to inhibit human complement and, therefore, promote human infection. This is based in previous work highlighting that even small amounts of variation at PFam54 and other loci can greatly influence protein function[14–18]. Additionally, we aimed to determine if variation at other PFam54 loci could be of functional relevance. Nucleotide diversity (π) provides a measure of variation across sequences allowing for easy quantification if diversity is present. Calculating ratios of synonymous and non-synonymous mutations (*dN/dS*) over all sequences allow us to determine if genes potentially differ in selective pressures suggesting divergence between the populations, and therefore, potential differences in population-specific protein function. This can then be used to inform protein structure prediction and determine if variation could impact protein function in later analyses.

No PFam54 genes were significantly higher or lower in terms of nucleotide diversity in either population (European lp54 π range, $\mu \pm 2xSD = 0.000–0.001$; Asian lp54 π range, $\mu \pm 2xSD = 0.000–0.031$), although Asian PFam54 orthologs always had higher nucleotide diversity (Fig. 1a, **Supplementary Table 3**). The majority of PFam54 orthologs displayed *dN/dS* ratios under 1.0 potentially signifying purifying selection (Fig. 1b, **Supplementary Table 3**). However, ratios where only significantly higher than the background ratios (*dN/dS* range, $\mu \pm 2xSD = 0.000–1.583.000.583$) in the case of *bga66* and *bga72*, which could suggest potential positive selection (Fig. 1b, **Supplementary Table 3**). In previous branch-based analyses however, diversifying selection at these genes was not observed[32]. Taken together, these findings support our hypothesis that genetic diversity is present in Asian isolates at PFam54 loci, including at genes of known function (*bga66*, *bga71*) which could have impacts on protein function. We aimed to study this further in two, focal Asian *B. bavariensis* isolates, NT24 and JHM1114. These isolates were chosen based on: (1) their unique PFam54 gene array architecture (Fig. 1c), and (2) their location within the overall *B. bavariensis* phylogeny (Fig. 1d), suggesting their inclusion could be representative for other Asian isolates.

For deciphering the complement-inhibitory function, we focused on Clade IV orthologs from NT24 and JHM1114 (*bga66-bga72*, *bga67b*, *bga68b*, *bga71b*)[13,32] as the orthologs of PBi (*bga66-bga72*) have been studied[25,60]. In addition to this, the crystal structure of $BGA71_{PBi}$ has already been determined[60]. This allows AlphaFold predicted structures of other Clade IV orthologs to be produced based on high structural similarity to BGA71 (RMSD value; 0.81–1.99 Å) (Fig. 2a-d), so as to test if variation could have functional relevance. All PFam54 proteins modeled here are entirely α-helical, composed of six α-helices (αA to αF) connected by short loop regions, except for the loop between αA and αB (Fig. 2a-d). According to SignalP-5.0[61], all Clade IV paralogs of *B. bavariensis* contains a signal sequence characteristic of lipoproteins. Following the signal sequence, a disordered loop region is present, which was not resolved in the crystal structure of $BGA71_{PBi}$ and was excluded from the AlphaFold predicted structures due to a very low confidence scores (pLDDT < 50) (Fig. 2b). Similar to the paralogs of PBi, the structural alignment of AlphaFold predicted structures showed high overall similarity among the Asian-specific Clade IV paralogs (RMSD value: 0.81–1.61 Å) (Fig. 2c-d). Sequence analyses of PFam54 Clade IV orthologs shared by the focal isolates showed amino acid substitutions in Asian isolates (JHM1114, NT24) when compared to PBi although the absolute number of substitutions differed between the respective orthologs (**Supplementary Figures S1a-h**).

In this analysis, we aimed to determine (1) if variation found in Asian isolates along proteins with known complement-inhibitory functions (BGA66, BGA71) is predicated to have functional impacts and (2) if variation along other Clade IV PFam54 orthologs in Asian isolates could suggest the presence of complement-inhibitory function. BGA71 orthologs of NT24 and JHM1114 displayed the highest number of amino acid substitutions in comparison to PBi (**Supplementary Figure S1a**). This included a conserved, nine amino acids long indel in $BGA71_{PBi}$ (residues 43–52) compared to NT24 and JHM1114, followed by a seven amino acid long variable region (**Supplementary Figure S1a, b**). Structural alignment of these BGA71 sequences revealed that the indel and variable region corresponds to a region suggested to have functional relevance in previous studies[25], but is present in the unstructured loop region excluded from our predicted structures (Fig. 3a). Apart from these

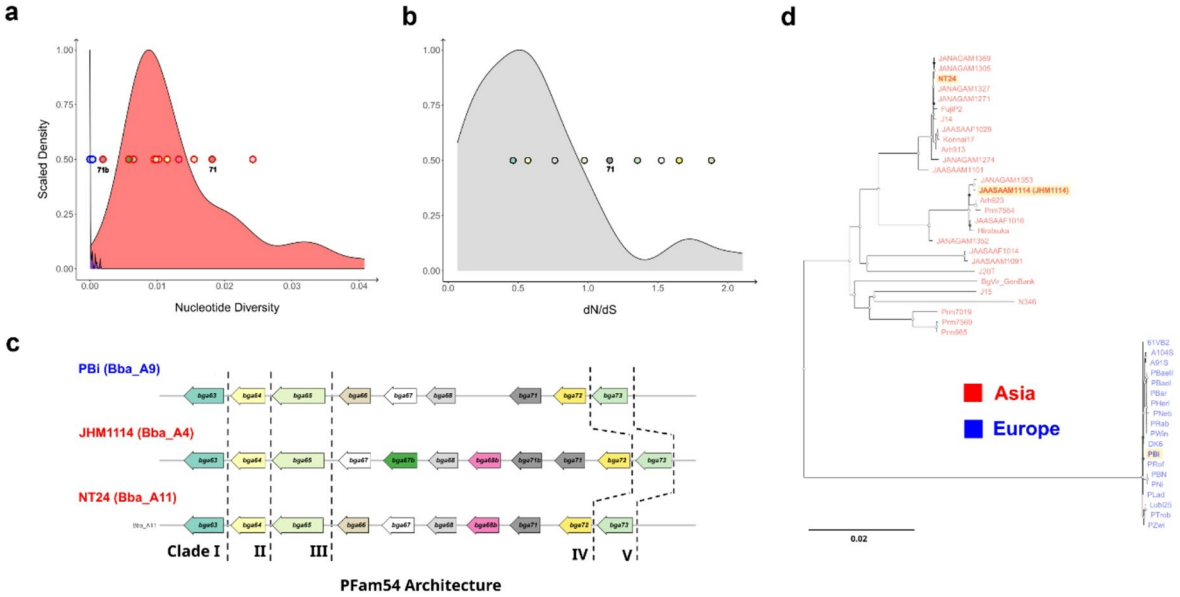

Fig. 1. Overview of the *Borrelia bavariensis* isolates used in the current study and description of the genetic diversity of PFam54 Clade IV orthologs. Nucleotide diversity (π) **(a)** and ratios of non-synonymous and synonymous (*dN/dS*) **(b)** of all PFam54 members (plotted points) of *B. bavariensis* isolates from Europe (blue) and Asia (red). Point color refers to the PFam54 genes orthology groups (OG) supported in[32]. As *bga71* and *bga71b* belong to the same OG (dark grey) they are labeled in both plots **(a**, **b)**. These values were calculated from all available sequences of each PFam54 ortholog from the previously published genomic data for European (n = 19) and Asian (n = 28) isolates[13,32], for individual values refer to Supplementary Table 3. Background distributions were determined based on all lp54-located genes (see Material and Methods). Estimation of π**(a)** was done per population (i.e., Asia or Europe) whereas *dN/dS***(b)** values were estimated for all samples across both populations. For this reason, *dN/dS* ratios could only be determined for genes present in both populations. **(c)** PFam54 architecture types of the focal isolates as described in[32]. Gene color corresponds to gene orthology between isolates and species as described previously[32]. The PFam54 architecture type for NT24 (Bba_A11), JHM1114 (Bba_A4), and PBi (Bba_A9) as determined in[32] are shown in parentheses next to the isolate name. **(d)** Phylogeny based on the lp54 plasmid sequence of *B. bavariensis* isolates as reported in[32]. The isolates chosen for functional validation in this study (NT24, JAASAAM1114, i.e., JHM1114, and PBi) are shown in bold. Nodes are colored by support probability with white representing a node probability of 1 and black referring to the lowest probability present in the tree of 0.57. The scale bar is in substitutions per base pair.

differences, the overall structure of all three orthologs ($BGA71_{PBi}$, $BGA71_{NT24}$, $BGA71_{JHM1114}$) remains highly conserved (RMSD value < 0.5 Å). Importantly, the surface-exposed cysteine at position 173 located on αD in $BGA71_{PBi}$, previously found to be involved in cross-linking two protomers to form a dimer and speculated to have some functional relevance[60], is conserved in all BGA71 orthologs (Fig. 3a **and Supplementary Fig. 1a**, **b**). Structural alignment of $BGA66_{PBi}$ and $BGA66_{NT24}$ (absent in JHM1114), revealed that 8 of 19 substitutions are located in the unstructured N-terminal loop region, while, of those located within the structural domain (11 substitutions), all are positioned on the solvent accessible protein surface (Fig. 3b and **Supplementary Figure S1c**). Taken together, this variation is present in relevant locations of the predicted structures suggesting that, hypothetically, impacts to protein functionality could be present.

For the other PFam54 orthologs shared between the populations, only structural analysis of BGA67 from PBi, NT24, and JHM1114 revealed that all 23 substitutions found in the structural domain are clustered relatively closely, primarily affecting αC (with 7 substitutions), along with the distal ends of αA and αE (Fig. 3c **and Supplementary Figure S1d**). With most residues being polar and facing the aqueous environment, this could suggest a potential role in protein functionality and therefore deviation from tested functions in European type strain PBi. This was not the case for residues in BGA68 and BGA72, although also being found predominantly in the structural domain (Fig. 3d-e). As for the novel Asian PFam54 orthologs (*bga67b*, *bga68b*, *bga71b*), variation is present among Asian isolates (**Supplementary Fig. 3b**, **f**, **h**) although what function the encoded proteins could have, is still not known. In the case of BGA71b, this protein shares many similarities to Asian BGA71 sequences suggesting that these two proteins could share similar functions. Both BGA67b and BGA68b, are orthologs of *B. garinii* proteins ZQA68 and ZQA70, respectively although substantial variation is present. Only ZQA68 has a known function, specifically binding avian FH, but as BGA67b contains a four amino acid long indel near the N-terminus and 26 amino acid substitutions it is likely that functionality here could differ (**Supplementary Figure S1h**). Indeed, structural analysis revealed that 22 substitutions were located in the structural domain and are clustered along αC and the loop region between αE and αF, but with a relatively conserved predicted structure (RMSD 0.69 Å) (Fig. 3f).

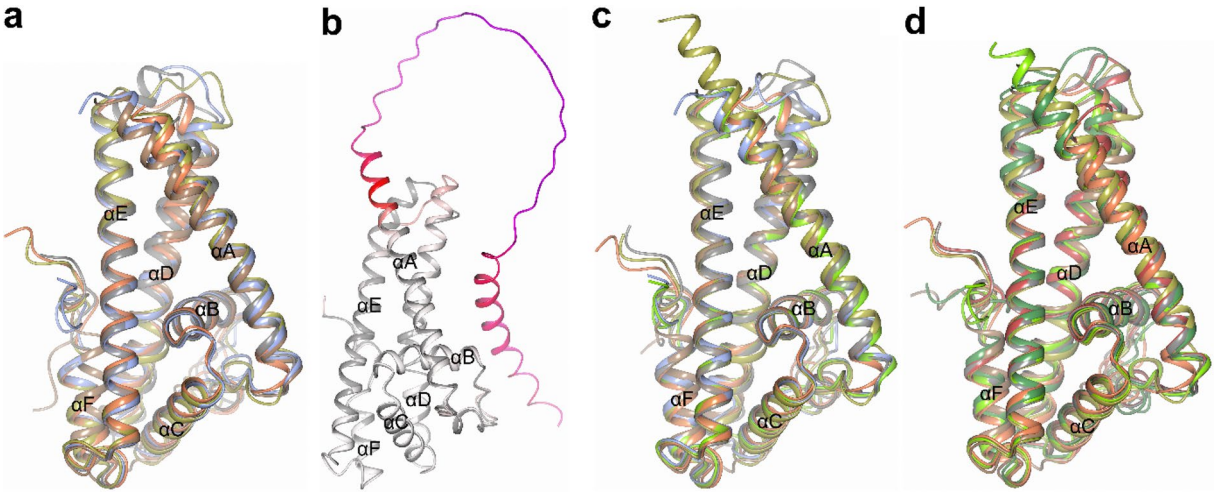

Fig. 2. Structural comparison of *B. bavariensis* PBi PFam54 Clade IV orthologs. **(a)** The crystal structure of *B. bavariensis* PBi orthologs $BGA71_{PBi}$ (gray; PDB ID 6FMH) superimposed with $BGA66_{PBi}$ (blue; RMSD 1.61 Å), $BGA67_{PBi}$ (gold; RMSD 1.56 Å), $BGA68_{PBi}$ (orange; RMSD 1.31 Å), and $BGA72_{PBi}$ (brown; RMSD 1.99 Å). **(b)** The crystal structure of $BGA71_{PBi}$ (gray; PDB ID 6FMH) superimposed with the full-length AlphaFold predicted structure of $BGA71_{PBi}$, colored according to the predicted local distance difference test (pLDDT), also known as a confidence score, where white indicates high confidence and red indicates low confidence. **(c)** The AlphaFold predicted structure of *B. bavariensis* NT24 orthologs $BGA66_{NT24}$ (blue) superimposed with $BGA67_{NT24}$ (gold; RMSD 1.23 Å), $BGA68_{NT24}$ (orange; RMSD 1.15 Å), $BGA68b_{NT24}$ (green; RMSD 0.81 Å), $BGA71_{NT24}$ (gray; RMSD 1.52 Å), and $BGA72_{NT24}$ (brown; RMSD 1.01 Å). **(d)** The AlphaFold predicted structure of *B. bavariensis* JHM1114 orthologs $BGA67b_{JHM1114}$ (gold) superimposed with $BGA67b_{JHM1114}$ (dark green; RMSD 1.58 Å), $BGA68_{JHM1114}$ (orange; RMSD 1.31 Å), $BGA68b_{JHM1114}$ (green; RMSD 1.25 Å), $BGA71_{JHM1114}$ (gray; RMSD 1.44 Å), $BGA71b_{JHM1114}$ (dark red; RMSD 1.41 Å), and $BGA72_{JHM1114}$ (brown; RMSD 1.61 Å). All six α-helices have been indicated from αA to αF.

In summary, analysis of genetic diversity and structural prediction of PFam54 orthologs derived from Asian isolates shows (1) substantial variation is present in proteins known to inhibit human complement (BGA66, BGA71) with proposed functional implications, (2) variation in genes with no known function in European type strain PBi that could have the potential to modify functionality in Asian isolates, and (3) variation in Asian-specific PFam54 proteins (BGA67b, BGA68b, and BGA71b) that could suggest some, or all, of these proteins may have unique complement-inhibitory function. We set out to test this through functional validation as described in the sections below.

Tick-derived Japanese *Borrelia bavariensis* NT24 and JHM1114 resist complement-mediated killing in human serum

Although tick-derived NT24 and JHM1114[13,19] belong to a phylogenetic clade (Fig. 1d) containing isolates with known human pathogenicity[10], which are hypothesized to be resistant to human complement as observed for PBi, no information is available, to the best of our knowledge, if the selected isolates are resistant to human complement. To initially determine the capability of Asian *B. bavariensis* isolates to resist complement, NT24 and JHM1114 were incubated in the presence of 50% non-immune human serum (NHS) or heat-inactivated serum (hiNHS). The survival of spirochetes was then documented by counting motile cells after 0, 2, 4, and 6 h by dark-field microscopy. As depicted in Fig. 4a, the majority of NT24 and JHM1114 spirochetes survived incubation for 6 h (73% and 63%, respectively) comparable with the type strain PBi while more than 90% of serum-sensitive *B. garinii* G1 spirochetes (control) were killed within 2 h. Growth of either *Borrelia* strain was unaffected when challenged with hiNHS (Fig. 4b). This finding indicates that NT24 and JHM1114 display a serum-resistant phenotype and overcome complement-mediated killing at comparable levels to those previously observed for European *B. bavariensis* strains including PBi used as a control for these analyses[25,28].

Impact of Asian PFam54 recombinant proteins on complement activation

Having demonstrated that NT24 and JHM1114 overcome human complement, we aimed to elucidate the molecular mechanisms of complement inhibition in more detail. As previously described, $BGA66_{PBi}$ and $BGA71_{PBi}$ inhibit TP activation by interacting with late complement components including C9 and thereby terminate MAC assembly[25]. Thus, we sought to assess the inhibitory potential of the respective orthologs of NT24 ($BGA66_{NT24}$, $BGA71_{NT24}$) as well as other PFam54 Clade IV encoded orthologs from NT24 and JHM1114 ($BGA67_{NT24}$, $BGA68_{NT24}$, $BGA68b_{NT24}$, $BGA67b_{JHM1114,}$ $BGA71b_{JHM1114}$) on complement activation and TP inhibition. Except $BGA67_{NT24}$ and $BGA68b_{NT24}$, all other orthologs could be produced in *E. coli* and purified by affinity chromatography. As a recombinant protein of BGA72 was not available from PBi for comparison, a recombinant protein of BGA72 from NT24 or JHM1114 could not be produced. Initially, we assess the complement inhibitory capacity on the AP and CP by employing ELISA-based assays[25,56]. LPS and IgM-coated

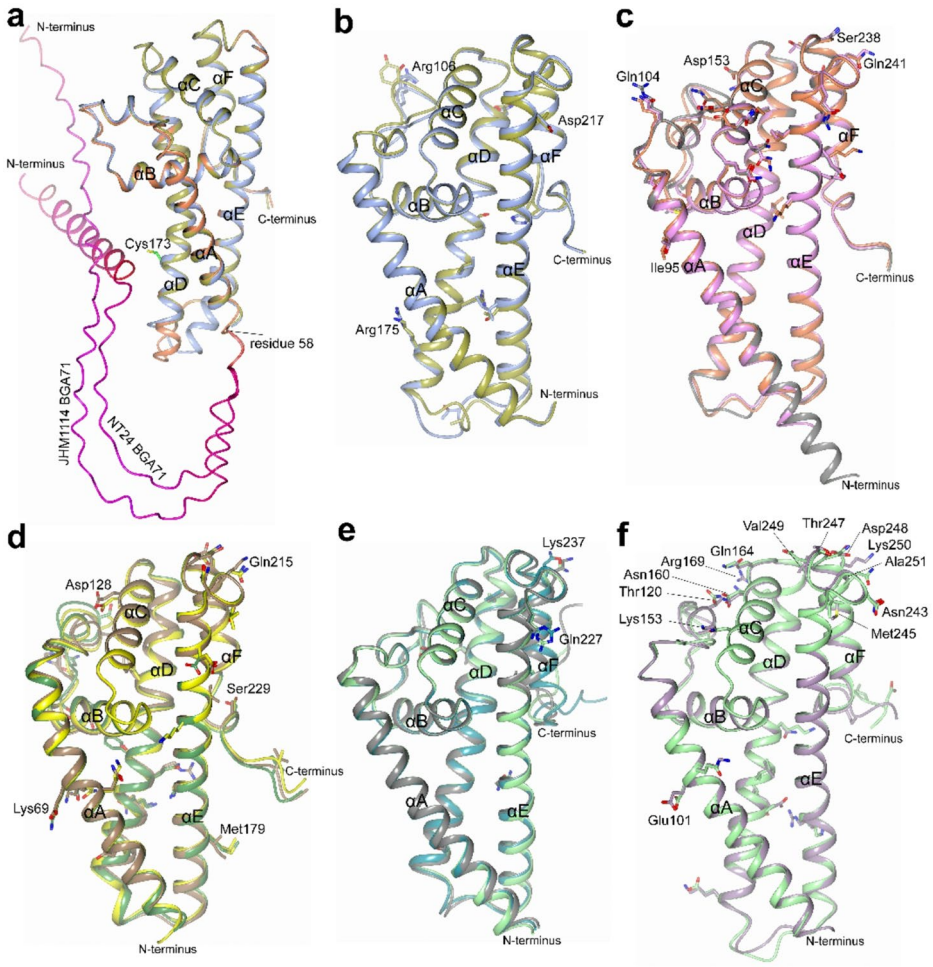

Fig. 3. Structure comparison of PFam54 Clade IV orthologs of Japanese *B. bavariensis* NT24 and JHM1114 with *B. bavariensis* PBi. **(a)** Superimposed crystal structure of $BGA71_{PBi}$ (blue; PDB ID 6FMH) with the predicted structures of $BGA71_{NT24}$ (gold; RMSD 0.43 Å) and $BGA71_{JHM1114}$ (orange; RMSD 0.42 Å). Residues 1–58 in $BGA71_{NT24}$ and $BGA71_{JHM1114}$ are coloured according to the confidence score, where white would indicate high confidence while red shows low confidence (pLDDT < 50). Cys173 in $BGA71_{PBi}$ has been indicated. **(b)** Superimposed predicted structures of $BGA66_{PBi}$ (blue) with $BGA66_{NT24}$ (gold; RMSD 0.60 Å). **(c)** Superimposed predicted structures of $BGA67_{PBi}$ (orange) with $BGA66_{NT24}$ (grey; RMSD 0.65 Å) and $BGA67b_{JHM1114}$ (pink; RMSD 0.67 Å). **(d)** Superimposed predicted structures of $BGA68_{PBi}$ (green) with $BGA68_{NT24}$ (yellow; RMSD 0.56 Å) and $BGA68_{JHM1114}$ (brown; RMSD 0.88 Å). **(e)** Superimposed predicted structures of $BGA72_{PBi}$ (grey) with $BGA72_{NT24}$ (green; RMSD 0.83 Å) and $BGA72_{JHM1114}$ (cyan; RMSD 0.63 Å). Residues affected by substitutions have been indicated for all three proteins as sticks and some of the residues in PBi that have been substituted in the other two strains have been indicated. **(f)** Structural comparison between $BGA67b_{JHM1114}$ (lilac) and ZQA68 from *B. garinii* ZQ1 (green; RMSD 0.69 Å). Some of the residues in $BGA67b_{JHM1114}$ have been indicted. All six α-helices have been indicated from αA to αF.

microtiter plates were incubated with reaction mixtures containing NHS pre-incubated with 4 µM of purified proteins and the formation of the MAC was detected by a neoepitope-specific antibody. As shown in Fig. 5a-b, none of the orthologs analyzed impacted activation of the AP and CP except partially by $BGA71b_{JHM1114}$ and fully by the control proteins $CspA_{B31}$ and $BBK32_{205}$. BSA did not inhibit complement activation. These findings indicate that almost all of the PFam54 orthologs originated from Asian *B. bavariensis* strains did not differ in their inhibitory activity on the AP and CP compared to $BGA66_{PBi}$, $BGA67_{PBi}$, $BGA68_{PBi}$, and $BGA71_{PBi}$ (Fig. 5a-b, **Supplementary Fig. 2a-b**)[25].

Assuming that the orthologs might affect TP activation as shown for $BGA66_{PBi}$ and $BGA71_{PBi}$[25], a hemolytic assay was conducted by using C5b-6 sensitized sheep erythrocytes. In parallel, reaction mixtures containing $BGA66_{NT24}$, $BGA71_{NT24}$, $BGA68_{NT24}$, $BGA67b_{JHM1114}$, and $BGA71b_{JHM1114}$ as well as control proteins $CspA_{B31}$, $BGA66_{PBi}$, and BSA were incubated with C7, C8, and C9. After incubation of the erythrocytes with the pre-incubated reaction mixtures, the release of hemoglobin was measured. Among the orthologs investigated, $BGA66_{NT24}$, $BGA67b_{JHM1114}$, and, in part, $BGA71b_{JHM1114}$ protected sheep erythrocytes from complement-mediated lysis in a dose dependent fashion (Fig. 5c). As expected, inhibition of MAC formation was also

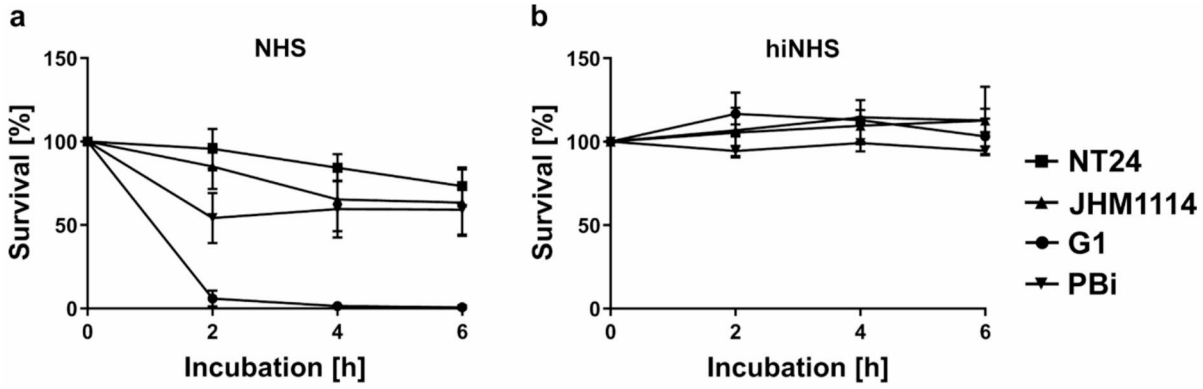

Fig. 4. *B. bavariensis* NT24 and JHM1114 resist complement-mediated killing in human serum. The percentage of motile cells of *B. bavariensis* NT24, JHM1114, PBi, and *B. garinii* G1 grown in either 50% NHS **(a)** or 50% hiNHS **(b)** were determined by dark-field microscopy at 0, 2, 4, and 6 h. At least three independent biological replicates were assayed for NHS-treated spirochetes and two independent biological replicates were conducted for hiNHS-treated cells. Each test gave similar results. For clarity, only data from a representative experiment is shown. Error bars indicate standard deviation (SD). For all plots, abbreviations refer to: NHS, non-immune human serum, hiNHS, heat-inactivated NHS.

observed for $BGA66_{PBi}$, $CspA_{B31}$, and vitronectin (Vn), the natural inhibitor of the MAC. In sum, $BGA66_{NT24}$, $BGA67b_{JHM1114}$, and potentially $BGA71b_{JHM1114,}$ but no other tested PFam54 protein, including $BGA71_{NT24,}$ inhibit activation of the TP.

Next, we determined if impairment of C9 polymerization directly correlates with TP inhibition as previously described in European *B. bavariensis*[25]. Naturally, monomeric C9 auto-polymerizes to high molecular weight homomers in the presence of divalent Zn^{2+}. To determine how PFam54 orthologs impact the auto-catalytic process, purified proteins at a concentration of 5 µg and 10 µg, respectively, were allowed to interact with monomeric C9 molecules (Fig. 5d **and e**). Controls included $BGA66_{PBi}$, $CspA_{B31}$, and purified C9 incubated with or without Zn^{2+}. Following initiation of C9 polymerization by adding 50 µM $ZnCl_2$, monomeric and polymeric C9 were visualized by silver staining. $BGA66_{NT24}$ and $BGA71_{NT24}$ inhibited C9 polymerization at 5 and/or 10 µg, respectively, while $BGA68_{NT24}$, $BGA67b_{JHM1114}$, and $BGA71b_{JHM1114}$ did not. To demonstrate whether $BGA66_{NT24}$ and $BGA66_{PBi}$ differ in their inhibitory capacity, a lower protein concentration of 2.5 µg was applied. Only $BGA66_{PBi}$ inhibited C9 polymerization in the presence of 2.5 µg and, therefore, more efficiently impacted C9 auto-polymerization compared to $BGA66_{NT24}$ (Fig. 5f). Structural comparison of these tested proteins revealed a high structural conservation (Fig. 6a). Comparison of proteins found to inhibit C9-polymerization ($BGA66_{NT24}$, $BGA71_{NT24}$, $BGA66_{PBi}$) uncovered conserved residues that could be involved in C9 polymerization inhibition clustered along αE (Fig. 6b) which were absent from proteins incapable of affecting C9-polymerization ($BGA68_{NT24}$, $BGA67b_{JHM1114}$, $BGA71b_{JHM1114}$) (Fig. 6a). Comparative analyses implementing loss-of-function variants in which single or multiple residues in αE are replaced will reinforce the conclusion drawn from the structure predictions.

In sum, our findings indicate that BGA66 orthologs derived from Asian and European isolates inhibit human complement by blocking the formation of the MAC whereas $BGA66_{PBi}$ appears to inhibit the TP more efficiently. In contrast to $BGA71_{PBi}$, $BGA71_{NT24}$ only partially affects C9 polymerization at higher concentrations without affecting TP inhibition. The orthologs of JHM1114 differ in their mode of complement inhibition as both proteins more ($BGA67b_{JHM1114}$) or less efficiently ($BGA71b_{JHM1114}$) block TP activation but did not impact C9 polymerization.

Ectopically producing PFam54 Clade IV orthologs of NT24 and JHM1114 confer serum resistance

Having demonstrated that PFam54 Clade IV orthologs $BGA66_{NT24}$, $BGA71_{NT24}$, $BGA67b_{JHM1114}$, and $BGA71b_{JHM1114}$ impacted complement in certain ways (Fig. 5), we next generated gain-of-function strains for examining the role of these particular proteins in facilitating complement resistance under more physiological conditions. Hence, the serum-sensitive *B. garinii* strain G1 was transformed with the respective shuttle vectors encoding for $BGA66_{NT24}$, $BGA71_{NT24}$, $BGA67b_{JHM1114}$, $BGA71b_{JHM1114}$, and $BGA68b_{NT24}$, respectively. $BGA68b_{NT24}$ was also included for these analyses due to the obstacle to produce recombinant protein in *E. coli*. *Borrelia garinii* G1 producing BGA66 or BGA71 from PBi were included as controls. Susceptibility of transformed *B. garinii* cells to human complement were then determined by incubating each strain with 50% NHS and 50% hiNHS for 2, 4, and 6 h. The majority of cells producing $BGA66_{NT24}$, $BGA67b_{JHM1114}$, $BGA71_{NT24}$, or $BGA71b_{JHM1114}$ survived after 6 h (Fig. 7), indicating that these proteins protect spirochetes from complement-mediated killing. Similarly, $BGA66_{PBi}$ and $BGA71_{PBi}$ enables serum resistance of surrogate *B. garinii* G1 but not $BGA67_{PBi}$ and $BGA68_{PBi}$ originated from PBi (**Supplementary Fig. 3**). By contrast, gain-of-function strains G1/$pBGA68b_{NT24}$, G1/$pBGA68b_{NT24}$, and G1/pKFSS1 (empty shuttle vector control) did not survive in NHS and the number of motile cells drastically declined to more than 90% after 2 h. As expected, treatment with hiNHS

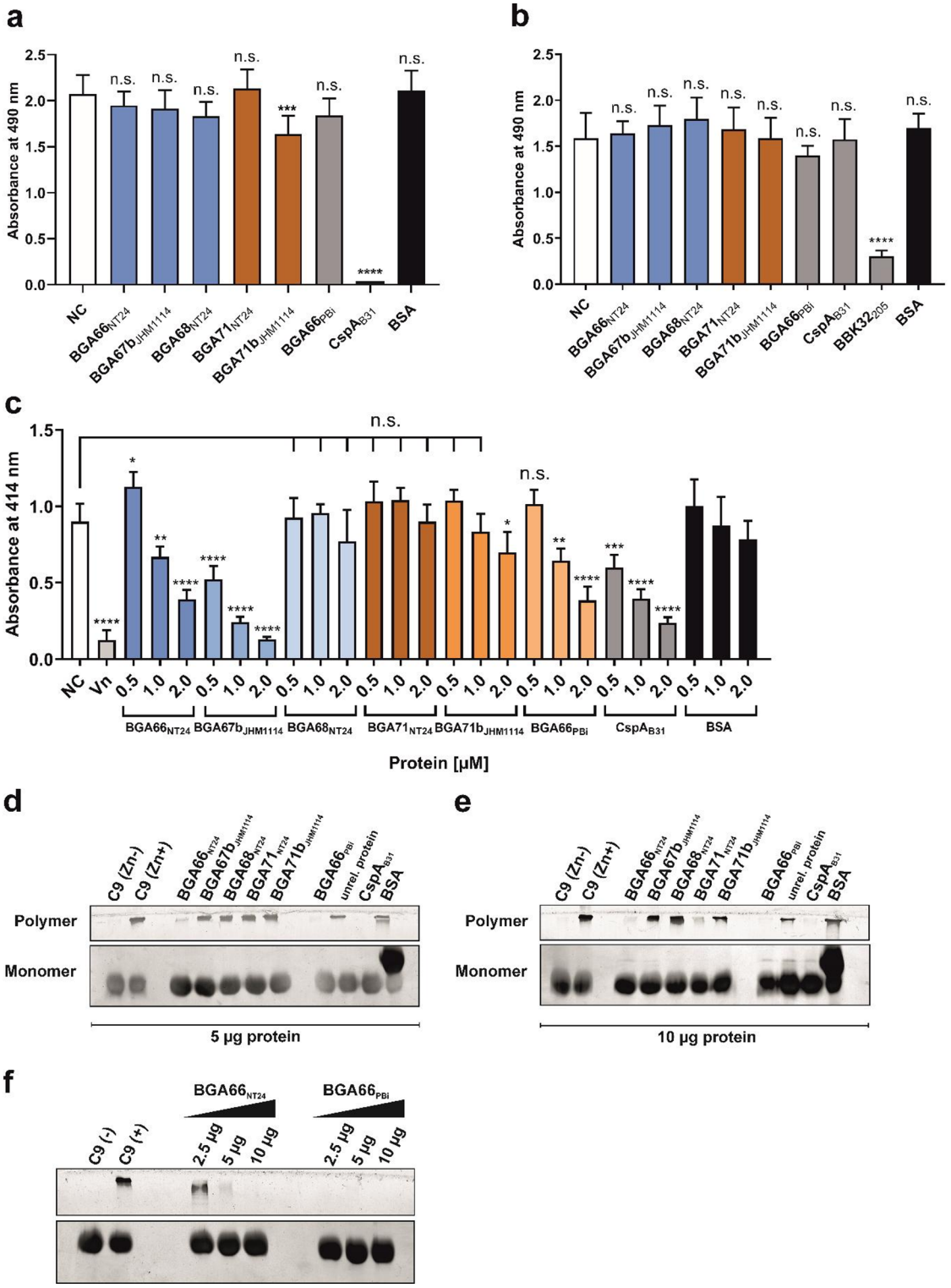

instead of NHS did not affect spirochetes motility as 90–100% of the cells survived over the whole incubation period.

Taken together, the data collected from the serum bactericidal assays demonstrate that both, BGA66$_{NT24}$ and BGA71$_{NT24}$ promote complement protection of serum-sensitive spirochetes similar to the counterparts derived from *B. bavariensis* PBi. These analyses also identify two novel but functional related orthologs, BGA67b$_{JHM1114}$ and BGA71b$_{JHM1114}$ exhibiting complement-inhibitory activity and facilitate serum resistance whereas BGA68$_{NT24}$ and BGA68b$_{NT24}$ lack complement-inhibitory properties as observed for BGA68$_{PBi}$.

Discussion

Borrelia bavariensis displays a unique demographic history having expanded into a novel location from an ancestral Asian population through a hypothesized invasion of the European tick vector, *I. ricinus*[4,11,13]. A

◂**Fig. 5**. Impact of PFam54 Clade IV orthologs of *B. bavariensis* NT24 and JHM1114 on complement activation and C9 polymerization. Assessment of the complement-inhibitory activity of PFam54 orthologs on the AP **(a)** and CP **(b)**. NHS pre-incubated with increasing concentrations of His_6-tagged borrelial proteins or BSA (control) were added to microtiter plates coated with either LPS (AP) or IgM (CP). To detect formation of the MAC, a neoepitope-specific, monoclonal anti-C5b-9 antibody (dilution 1:500) was used. All experiments were performed at least three times, with each individual test carried out in triplicate. Raw data were analyzed using one-way ANOVA with Bonferroni post-hoc test (confidence interval = 95%). ****, $p \leq 0.0001$; ***, $p < 0.001$;, *, $p < 0.05$, n.s., no statistical significance. **(c)** Determination of the complement-inhibitory activity of PFam54 orthologs on the TP. C5b-6-sensitized sheep erythrocytes were incubated with mixtures containing C7, C8, and C9 and the purified His_6-tagged proteins or BSA. Absorbance values at 414 nm indicate hemolysis of erythrocytes. Data represent means of three independent experiments and error bars correspond to SD. Raw data were analyzed using one-way ANOVA with Bonferroni post-hoc test (confidence interval = 95%). ****, $p \leq 0.0001$; ***, $p < 0.001$; **, $p < 0.01$; *, $p < 0.05$. NC, negative control; Vn, vitronectin. **(d** and **e)** Impact of PFam54 orthologs on C9 polymerization. His_6-tagged proteins or BSA were incubated with C9 and polymerization of C9 was initiated by adding 50 µM $ZnCl_2$. After separation of the reaction mixtures through 7.5% SDS gels, monomeric and polymeric C9 were visualized by silver staining. **(f)** Impact of BGA66 orthologs on C9 polymerization. C9 was incubated with increasing concentrations of His_6-tagged proteins. NC, negative control.

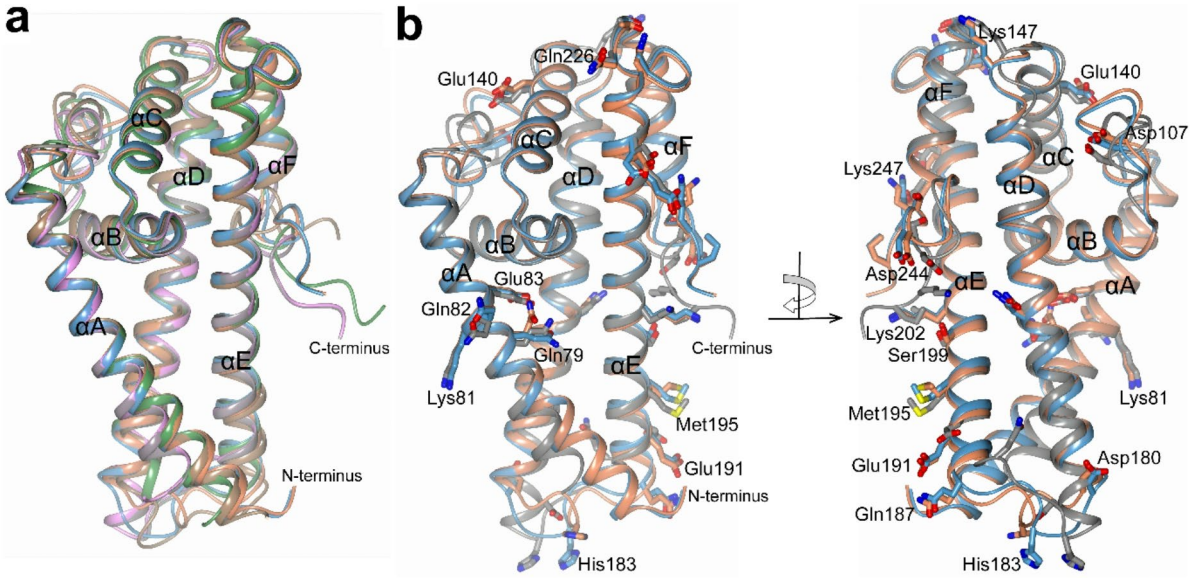

Fig. 6. Localization of the potential C9 interacting region within PFam54 Clade IV orthologs. **(a)** Superimposed predicted structure of $BGA66_{PBi}$ (blue) with $BGA66_{NT24}$ (orange; RMSD 0.60 Å), $BGA68_{NT24}$ (green; RMSD 1.26 Å), $BGA71_{NT24}$ (gray; RMSD 1.49 Å), $BGA67b_{JHM1114}$ (brown; RMSD 1.52 Å), and $BGA71b_{JHM1114}$ (pink; RMSD 1.46 Å). **(b)** Superimposed $BGA66_{PBi}$ (blue) with $BGA66_{NT24}$ (orange; RMSD 0.60 Å) and $BGA71_{NT24}$ (gray; RMSD 1.49 Å) showing the conserved residues between the three members, but not with $BGA68_{NT24}$, $BGA67b_{JHM1114}$, and $BGA71b_{JHM1114}$. The structure is showed in two different angles, rotated by 180 degrees. All six α-helices have been indicated from αA to αF.

byproduct of this adaptive event is, European isolates exhibiting a marked tropism for neurological tissues which appears absent in Asian isolates[5,10]. Here, we aimed to determine if naturally occurring genetic variation affects the human complement inhibitory properties of PFam54 orthologs originated from Asian *B. bavariensis* isolates and if complement inhibition could be a trait unique to European isolates, potentially influencing the observed differences in infection phenotypes. Previous data convincingly showed that even little variation along functionally relevant proteins can substantially impact various *Borrelia* species (*B. burgdorferi*, *B. afzelii*) survival during various portions of the transmission cycle[14–18]. Here, the PFam54 orthologs of NT24 and JHM1114 ($BGA66_{NT24}$, $BGA68_{NT24}$, $BGA71_{NT24}$, $BGA67b_{JHM1114}$, $BGA68b_{NT24}$, $BGA71b_{JHM1114}$) did display high genetic variation but with conservation of the overall protein fold. Likely due to this, biological function of the Asian orthologs remained similar compared to those derived from PBi[25]. This suggests that the complement-inhibitory function described for $BGA66_{PBi}$ and $BGA71_{PBi}$ is not a derived trait of European isolates and that complement inhibition alone is not sufficient to explain the differences observed in neurotropism of human infections between the *B. bavariensis* populations[5,10].

Despite the observed variation within the PFam54 gene family between European and Asian isolates[13,19,32], both Asian *B. bavariensis* isolates survived in complement-active NHS (Fig. 4). This supports that human

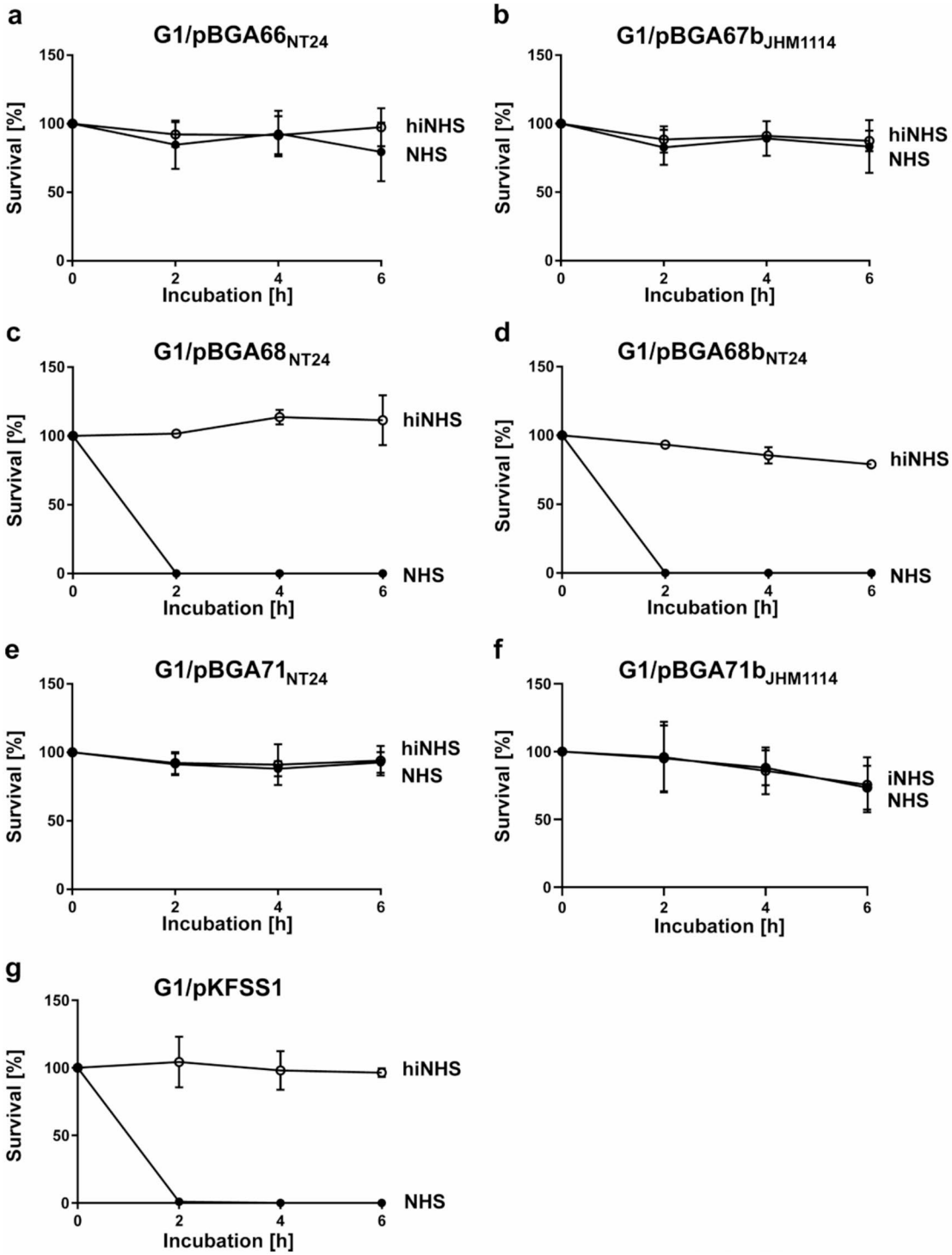

Fig. 7. PFam54 Clade IV orthologs of Asian *B. bavariensis* facilitates serum resistance in a gain-of-function *B. garinii* strain. Survival of *B. garinii* G1 containing vectors encoding for $BGA66_{NT24}$**(a)**, $BGA67b_{JHM1114}$**(b)**, $BGA68_{NT24}$**(c)**, $BGA68b_{NT24}$**(d)**, $BGA71_{NT24}$**(e)**, $BGA71b_{JHM1114}$**(f)**, and G1 carrying the empty shuttle vector **(g)** in 50% NHS (filled circles) or in 50% hiNHS (open circles) was monitored by dark-field microscopy. Motile cells were counted at 0, 2, 4 and 6 h. At least three independent biological replicates were conducted for treatments with NHS and two independent treatments with hiNHS. Error bars indicate ± SD. For all plots, abbreviations refer to: NHS, non-immune human serum, hiNHS, heat-inactivated NHS.

complement resistance is not unique to the European *B. bavariensis* population but is a characteristic feature of the whole species. As these geographically separated populations display an identical serum resistant phenotype, it is tempting to speculate that other, yet, unknown factors determine the observed differences in bacterial infectivity and clinical manifestations[5,10]. As previously stated, it has been observed that Asian *B. bavariensis* isolates do not display the same level of neurotropism as observed in European isolates, and thus present less often in neuroborreliosis cases throughout Asia[5,10]. Recent findings however suggest that the number of neuroborreliosis cases in Japan are underestimated and could be higher than previously thought[62]. It remains unclear which *Borrelia* species could be the causative agent of these LB cases as other neurotropic species, such as *B. garinii*[2], coexist with *B. bavariensis* in Asia. These two *Borrelia* species are sister taxa, with *B. bavariensis* being historically classified as a subtype of *B. garinii* associated with rodents before it was designated as a distinct species[12,63]. They both are capable of causing human LB, but with *B. garinii* showing a marked tropism for neurological tissues across its Eurasian range while only European *B. bavariensis* show this tropism as previously stated[5,10,64]. Recent analysis has also shown, that even though both these species share Asian origins, establishing into Europe was only adaptive in *B. bavariensis*[13] suggesting that they could differ in their ancestral capacity for human infection. Further study is required to determine what species is responsible for these reported neuroborreliosis cases.

To understand how PFam54-encoded proteins promote immune evasion, we initially compared BGA66 and BGA71, which show clear orthology between European and Asian isolates[32]. These proteins are suggested to possess similar complement-inhibitory properties in both *B. bavariensis* populations. $BGA66_{NT24}$ and $BGA66_{PBi}$ did show high similarity in overall protein fold (RMSD 0.60 Å) suggesting a complement-inhibitory potential for $BGA66_{NT24}$. Subsequent functional analyses confirmed the complement-inhibitory function of $BGA66_{NT24}$, although with reduced efficiency in preventing C9 polymerization (5 µg for $BGA66_{NT24}$ vs. <2.5 µg $BGA66_{PBi}$) (Fig. 5f). Even so, $BGA66_{NT24}$ conferred human serum resistance when ectopically produced (Fig. 7) indicating an important role in complement evasion. As our sequence analysis suggested BGA66 could be under positive selection (**Table 1**) this difference in efficiency could result from the demographic history of the European population[4,11,13,19], but it is important to note that branch-specific analyses did not find signatures of diversifying selection on this loci[32]. Like $BGA71_{PBi}$, both Asian orthologs ($BGA71_{NT24}$ and $BGA71b_{JHM1114}$) conferred resistance to human serum when ectopically produced (Fig. 7). As shown, *bga71b* most likely has arisen through recent gene duplication of *bga71*[32], suggesting that BGA71b and BGA71 could share similar functionality. Even so, functional differences were found between $BGA71_{PBi}$ and the Asian orthologs $BGA71_{NT24}$ and $BGA71b_{JHM1114}$, but also between the Asian orthologs. $BGA71_{NT24}$ and $BGA71b_{JHM1114}$ did not or only partially inhibited the TP (Fig. 5c **and Supplementary Fig. 2c**). By assaying these BGA71 orthologs, $BGA71_{NT24}$ did display an inhibitory capacity on C9 polymerization at higher concentrations (10 µg = 7.5 µM) in a similar way to $BGA71_{PBi}$[25] but $BGA71b_{JHM1114}$ did not (Fig. 5e). Regarding $BGA71_{NT24}$, it seems that 2.0 µM of purified protein used by default for the hemolytical assays are too low to achieve similar levels of inhibitory capacity on the TP compared to $BGA71_{PBi}$. Also, it is tempting to speculate whether a lower C9 binding affinity of $BGA71_{NT24}$ might account for the requirement of higher protein concentrations for TP inhibition or if $BGA71_{NT24}$ lacks additional binding activity to C7 and C8 as previously shown for $BGA71_{PBi}$[25]. Future studies are warranted to explore the molecular mechanism of how $BGA71_{NT24}$ inhibit complement and protect Asian *B. bavariensis* from complement-mediated killing. By sequence comparison, a deletion of up to 11 amino acids (41-ADPLNKKNQNF-52) has been identified at the N-terminus of $BGA71_{NT24}$ and all BGA71/BGA71b orthologs analysed so far from other Asian isolates (**Supplementary Fig. 1a-b**). Structure predictions of $BGA71_{PBi}$, $BGA71_{NT24}$ and $BGA71_{JHM1114}$ revealed that this specific amino acid stretch is located within the unstructured N-terminal loop region (Fig. 3a) previously identified in $BGA71_{PBi}$ to play a potential role for TP inactivation[25]. Although no structural information of the N-terminal region could be gathered by the AlphaFold2 predictions, it seems plausible that additional parts of BGA71 are relevant to mediate complement evasion as both, $BGA71_{NT24}$ and $BGA71b_{JHM1114}$, conferred resistance to human immune serum (Fig. 7e **and f**) and as the predicted protein structure of these BGA71 orthologs is well conserved (RMSD ~ 0.40 Å) (Fig. 3a). Overall, our findings suggest that the complement-inhibitory capacity of BGA66 and BGA71orthologs originating from Asian and European populations are comparable, but the underlying molecular mechanisms and efficiency of complement inhibition differs between the populations.

We further set out to determine if any other complement-inhibitory function was present in known or novel PFam54 Clade IV proteins present in *B. bavariensis* isolates NT24 and JHM1114. As already shown for the PBi[25], none of the PFam54 Clade IV proteins produced from NT24 and JHM1114 bound human Factor H as shown for CspA from *B. burgdorferi* (Fig. 2 **and Supplementary Fig. 4**) suggesting that Asian *B. bavariensis* possess similar strategies for evading human complement like European *B. bavariensis* isolates[25], also supported by the already discussed results. In our attempts to study additional PFam54 Clade IV orthologs, it is important to note that despite extensive efforts, we were unable to overproduce $BGA67_{NT24}$ and $BGA68b_{NT24}$ for functional analyses. By assaying the respective orthologs in *B. bavariensis* PBi, $BGA67_{PBi}$ was unable to protect serum-sensitive spirochetes from complement-mediated killing by human serum and did not inhibit C9 polymerization (**Supplementary Fig. 3b-d**). Due to high structural similarity of BGA67 orthologs originating from the Asian isolates and PBi (Figs. 2 and 3, **and Supplementary Fig. 1d**) it could be proposed that the $BGA67_{NT24}$ also would be unable to protect spirochetes from complement-mediated killing. Even so, $BGA67_{NT24}$ did display a clustering of residues in structural predictions (Fig. 3c **and Supplementary Fig. 1 d)** which could highlight a difference in functionality. Regarding BGA68b, we were able to generate a gain-of-function strain but the ectopically produced protein did not confer serum resistance (Fig. 7d), suggesting that this particular ortholog does not play a role in complement evasion. Overall, we cannot completely exclude that, additional factors such as protein expression levels, surface localization, or cooperative interactions with other borrelial proteins may contribute to serum resistance.

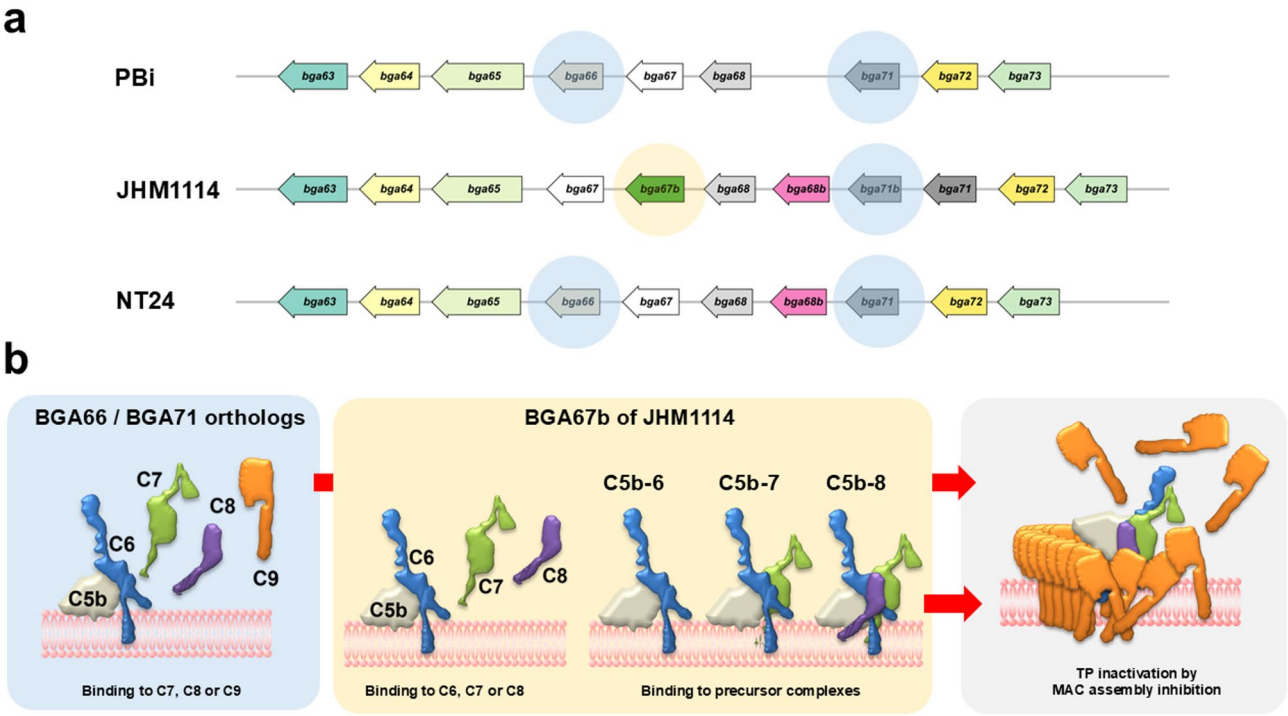

Fig. 8. Proposed mechanism of complement inhibition mediated by BGA orthologs of Asian *B. bavariensis* NT24 and JHM1114. PFam54 architecture of *B. bavariensis* isolates PBi, JHM1114, and NT24 as described in Fig. 1c **(a)**. Concept of the molecular mechanisms of complement interaction and inhibition mediated by BGA orthologs described in this study **(b)**.

Our comparative analyses with purified BGA67b$_{JHM1114}$ and BGA68$_{NT24}$ revealed a strong difference in their properties to affect complement as BGA68$_{NT24}$ displayed no inhibition, while BGA67b$_{JHM1114}$ displayed the strongest inhibition of the TP among all tested proteins, but without affecting C9 polymerization (Fig. 5c **and d**). This finding suggests that BGA67b$_{JHM1114}$ inhibits MAC assembly independently from C9 binding and is capable of conferring serum resistance (Fig. 7b). Therefore, some Asian isolates (~ 20%) possess an unique PFam54 ortholog, BGA67b[32], absent in European *B. bavariensis* strains and, here, identified as an inhibitor of the TP. Previously, we showed that the BGA67b is an ortholog of ZQA68 of *B. garinii* known to specifically inhibit complement-mediated killing by binding avian FH in birds[15,16]. These studies clearly demonstrated specific roles of this ortholog in facilitating resistance to avian but not to human serum. In line with this, BGA67b$_{JHM1114}$ was unable to bind human FH as shown for ZQA68 (**Supplementary Fig. 4**). Despite structural similarities to BGA67b$_{JHM1114}$ (RMSD 0.69 Å) (Fig. 3f), ZQA68 lacks inhibitory properties to human complement[15,16] suggesting that variation along BGA67b results in the unique ability observed here to confer complement resistance and inhibit the TP. Considering that most of the non-conserved residues between the two proteins are located at the distal end, it is likely that this region also serves as a binding site for a, yet unknown, interacting protein with BGA67b$_{JHM1114}$ (Fig. 3f).

In summary, our data support the notion that functionality of PFam54 Clade IV *B. bavariensis* orthologs remains stable across both Asian and European populations even though substantial inter-population variation exists[13,19,28,32]. This is in contrast to other work which has shown that even minor genetic variation along genes (e.g., *cspA*, *cspZ*) in various *Borrelia* species (*B. burgdorferi* and *B. afzelii*) could have a major impact on vector-to-host transmission, host-to pathogen-acquisition, pathogen dissemination or even host specialization and adaptation[14–18]. Whether such variations directly affect the ability of spirochetes to cause human LB remains a subject of ongoing debate. Taken together, our results demonstrated that Asian *B. bavariensis* isolates naturally resist complement-mediated killing potentially through conserved molecular mechanisms already described for the European isolates but also through novel interactions. Apart from the known mechanism facilitating serum resistance of *B. bavariensis*, e.g. targeting the TP by interacting with late complement components to prevent MAC assembly (BGA66 and BGA71 orthologs), inactivation of complement independently take place from acquisition of complement regulators or affecting the TP (BGA67b$_{JHM1114}$) (Fig. 8). Whether BGA67b$_{JHM1114}$ directly interacts with other components of the TP (e.g. C6, C7 or C8) or by binding to precursor MAC complexes C5b-6, C5b-7 or C5b-8 is a matter of further investigations.

Data availability

All data generated or analysed during this study are included in this published article (and its Supplementary Information files).

Received: 4 November 2025; Accepted: 5 March 2026
Published online: 13 March 2026

References

1. Kurtenbach, K. et al. Fundamental processes in the evolutionary ecology of Lyme borreliosis. *Nat. Rev. Microbiol.* **4**, 660–669 (2006).
2. Steere, A. C. et al. Lyme borreliosis. *Nat. Rev. Dis. Primers* **2**, 16090 (2016).
3. Maraspin, V., Ruzic-Sabljic, E. & Strle, F. Lyme borreliosis and *Borrelia spielmanii*. *Emerg. Infect. Dis.* **12**1177. (2006).
4. Margos, G., Fingerle, V. & Reynolds, S. *Borrelia bavariensis*: Vector switch, niche invasion, and geographical spread of a tick-borne bacterial parasite. *Front. Ecol. Evol.* **7**, 1–20 (2019).
5. Wilske, B. et al. Diversity of OspA and OspC among cerebrospinal fluid isolates of *Borrelia burgdorferi* sensu lato from patients with neuroborreliosis in Germany. *Med. Microbiol. Immunol.* **184**, 195–201 (1996).
6. Margos, G. et al. *Borrelia* Ecology, Evolution, and Human Disease: A Mosaic of Life. In *Zoonoses: Infections Affecting Humans and Animals* (eds Sing, A. et al.) 1087–1151 (Springer International Publishing, 2023). https://doi.org/10.1007/978-3-031-27164-9_49.
7. Steere, A. C., Coburn, J. & Glickstein, L. The emergence of Lyme disease. *J. Clin. Invest.* **113**, 1093–1101 (2004).
8. Fingerle, V. et al. Epidemiological aspects and molecular characterization of *Borrelia burgdorferi* s.l. from southern Germany with special respect to the new species *Borrelia spielmanii* sp. nov. *Int. J. Med. Microbiol.* **298**, 279–290 (2008).
9. Marconi, R. T. et al. Genetic analysis of *Borrelia garinii* OspA serotype 4 strains associated with neuroborreliosis: Evidence for extensive genetic homogeneity. *J. Clin. Microbiol.* **37**, 3965–3970 (1999).
10. Takano, A. et al. Multilocus sequence typing implicates rodents as the main reservoir host of human-pathogenic *Borrelia garinii* in Japan. *J. Clin. Microbiol.* **49**, 2035–2039 (2011).
11. Gatzmann, F. et al. NGS population genetics analyses reveal divergent evolution of a Lyme borreliosis agent in Europe and Asia. *Ticks Tick Borne Dis.* **6**, 344–351 (2015).
12. Margos, G. et al. Borrelia bavariensis sp. nov. is widely distributed in Europe and Asia. *Int. J. Syst. Evol. Microbiol.* **63**, 4284–4288 (2013).
13. Rollins, R. E. et al. Out of Asia? Expansion of Eurasian Lyme borreliosis causing genospecies display unique evolutionary trajectories. *Mol. Ecol.* **32**, 786–799 (2023).
14. Benoit, V. M., Fischer, J. R., Lin, Y. P., Parveen, N. & Leong, J. M. Allelic variation of the Lyme disease spirochete adhesin DbpA influences spirochetal binding to decorin, dermatan sulfate, and mammalian cells. *Infect. Immun.* **79**, 3501–3509 (2011).
15. Hart, T. et al. Polymorphic factor H-binding activity of CspA protects Lyme borreliae from the host complement in feeding ticks to facilitate tick- to-host transmission. *PLoS Pathog.* **14**, e1007105–e1007105 (2018).
16. Hart, T. et al. Host tropism determination by convergent evolution of immunological evasion in the Lyme disease system. *PLoS Pathog.* **17**, 1–29 (2021).
17. Lin, Y. P. et al. Strain-specific variation of the decorin-binding adhesin DbpA influences the tissue tropism of the Lyme disease spirochete. *PLoS Pathog.* **10**, e1004238–e1004238 (2014).
18. Marcinkiewicz, A. L. et al. Structural evolution of an immune evasion determinant shapes pathogen host tropism. *Proceedings of the National Academy of Sciences* 120, e2301549120–e2301549120 (2023).
19. Becker, N. S. et al. High conservation combined with high plasticity: Genomics and evolution of *Borrelia bavariensis*. *BMC Genom.* **21**, 702 (2020).
20. Atkinson, J. P. et al. 21 - The Human Complement System: Basic Concepts and Clinical Relevance. in *Clinical Immunology (Fifth Edition)* (eds Rich, R. R. et al.)Elsevier, London, 299–317.e1 (2019). https://doi.org/10.1016/B978-0-7020-6896-6.00021-1
21. Coburn, J. et al. Lyme disease pathogenesis. *Curr. Issues. Mol. Biol.* **42**, 473–518 (2021).
22. Kraiczy, P. Hide and seek: How Lyme disease spirochetes overcome complement attack. *Front. Immunol.* **7**, 385 (2016).
23. Skare, J. T. & Garcia, B. L. Complement Evasion by Lyme Disease Spirochetes. *Trends Microbiol.* **28**, 889–899 (2020).
24. Hallström, T. et al. CspA from Borrelia burgdorferi Inhibits the Terminal Complement Pathway. *mBio* **4** https://doi.org/10.1128/mbio.00481-13 (2013).
25. Hammerschmidt, C. et al. BGA66 and BGA71 facilitate complement resistance of *Borrelia bavariensis* by inhibiting assembly of the membrane attack complex. *Mol. Microbiol.* **99**, 407–424 (2016).
26. Kraiczy, P. & Stevenson, B. Complement regulator-acquiring surface proteins of *Borrelia burgdorferi*: Structure, function and regulation of gene experession. *Ticks Tick-borne Dis.* **4**, 26–34 (2013).
27. Schmit, V. L., Patton, T. G., Gilmore, R. D. J., Patton, V. L. S. & Gilmore, R. D. J. Analysis of *Borrelia burgdorferi* surface proteins as determinants in establishing host cell interactions. *Front. Microbiol.* **2**, 1–8 (2011).
28. Rollins, R. E. et al. Utilizing Two *Borrelia bavariensis* Isolates Naturally Lacking the PFam54 Gene Array To Elucidate the Roles of PFam54-Encoded Proteins. *Appl. Environ. Microbiol.* **88**, e01555–e01521 (2022).
29. Akther, S. et al. Natural selection and recombination at host-interacting lipoprotein loci drive genome diversification of Lyme disease and related bacteria. *mBio* **15**, e01749–e01724 (2024).
30. Schwartz, I., Margos, G., Casjens, S. R., Qiu, W. G. & Eggers, C. H. Multipartite genome of Lyme disease *Borrelia*: Structure, variation and prophages. *Curr. Issues. Mol. Biol.* **42**, 409–454 (2021).
31. Wywial, E. et al. Fast, adaptive evolution at a bacterial host-resistance locus: The PFam54 gene array in *Borrelia burgdorferi*. *Gene* **445**, 26–37 (2009).
32. Wülbern, J. et al. Unprecedented genetic variability of PFam54 paralogs among Eurasian Lyme borreliosis-causing spirochetes. *Ecol. Evol.* **14**, e11397–e11397 (2024).
33. Aziz, R. K. et al. The RAST Server: rapid annotations using subsystems technology. *BMC Genom.* **9**, 75–75 (2008).
34. Overbeek, R. et al. The SEED and the Rapid Annotation of microbial genomes using Subsystems Technology (RAST). *Nucleic Acids Res.* **42**, D206–D214 (2014).
35. R Core Team. *R: A language and environment for statistical computing* (R Foundation for Statistical Computing, 2024).
36. Ullrich, K. CRBHits: From Conditional Reciprocal Best Hits to codon alignments and Ka/Ks in R. *J. Open Source Softw.* **5**, 2424–2424 (2020).
37. Haas, B. J., Delcher, A. L., Wortman, J. R. & Salzberg, S. L. DAGchainer: A tool for mining segmental genome duplications and synteny. *Bioinformatics* **20**, 3643–3646 (2004).
38. Csárdi, G. & Nepusz, T. The igraph software package for complex network research. *Inter. J. Complex. Systems* **1695** (2006). https://igraph.org
39. Edgar, R. C. MUSCLE: A multiple sequence alignment method with reduced time and space complexity. *BMC Bioinformatics* **5**, 113–113 (2004).
40. Edgar, R. C. MUSCLE: Multiple sequence alignment with high accuracy and high throughput. *Nucleic Acids Res.* **32**, 1792–1797 (2004).
41. Nei, M. *Molecular Evolutionary Genetics* (Columbia University Press, 1987).
42. Paradis, E. Pegas: An R package for population genetics with an integrated-modular approach. *Bioinformatics* **26**, 419–420 (2010).
43. Charif, D. & Lobry, J. R. SeqinR 1.0–2: A Contributed Package to the R Project for Statistical Computing Devoted to Biological Sequences Retrieval and Analysis In (eds Bastolla, U. et al.) (2007).

44. Gouy, M., Milleret, F., Mugnier, C., Jacobzone, M. & Gautier, C. ACNUC: A nucleic acid sequence data base and analysis system. *Nucleic Acids Res.* **12**, 121–127 (1984).
45. Hu, C. M., Wilske, B., Fingerle, V., Lobet, Y. & Gern, L. Transmission of *Borrelia garinii* OspA serotype 4 to BALB/c mice by *Ixodes ricinus* ticks collected in the field. *J. Clin. Microbiol.* **39**, 1169–1171 (2001).
46. Huegli, D., Hu, C. M., Humair, P.-F., Wilske, B. & Gern, L. Apodemus species mice are reservoir hosts of *Borrelia garinii* OspA serotype 4 in Switzerland. *J. Clin. Microbiol.* **40**, 4735–4737 (2002).
47. Larsson, A. AliView: A fast and lightweight alignment viewer and editor for large datasets. *Bioinformatics* **30**, 3276–3278 (2014).
48. Robert, X. & Gouet, P. Deciphering key features in protein structures with the new ENDscript server. *Nucleic Acids Res.* **42**, W320–W324 (2014).
49. Siegel, C. et al. Deciphering the ligand-binding sites in the *Borrelia burgdorferi* complement regulator-acquiring surface protein 2 required for interactions with the human immune regulators factor H and factor H-like protein 1. *J. Biol. Chem.* **283**, 34855–34863 (2008).
50. Hammerschmidt, C. et al. Versatile roles of CspA orthologs in complement inactivation of serum-resistant Lyme disease spirochetes. *Infect. Immun.* **82**, 380–392 (2014).
51. Koenigs, A. et al. BBA70 of *Borrelia burgdorferi* is a novel plasminogen-binding protein. *J. Biol. Chem.* **288**, 25229–25243 (2013).
52. Schmidt, F. L. et al. Interaction between *Borrelia miyamotoi* variable major proteins Vlp15/16 and Vlp18 with plasminogen and complement. *Sci. Rep.* **11**, 4964–4964 (2021).
53. Nguyen, N. T. T. et al. The complement binding and inhibitory protein CbiA of *Borrelia miyamotoi* degrades extracellular matrix components by interacting with plasmin(ogen). *Front. Cell. Infect. Microbiol.* **8**, 23. https://doi.org/10.3389/fcimb.2018.00023 (2018).
54. Frank, K. L., Bundle, S. F., Kresge, M. E., Eggers, C. H. & Samuels, S. D. aadA confers streptomycin resistance in *Borrelia burgdorferi*. *J. Bacteriol.* **185**, 6723–6727 (2003).
55. Kraiczy, P., Skerka, C., Brade, V. & Peter, F. Further Characterization of Complement Regulator-Acquiring Surface Proteins of *Borrelia burgdorferi*. *Infect. Immun.* **69**, 7800–7809 (2001).
56. Damm, A.-S. et al. Multifunctional interaction of CihC/FbpC orthologs of relapsing fever spirochetes with host-derived proteins involved in adhesion, fibrinolysis, and complement evasion. *Front. Immunol.* **15**, 1390468. https://doi.org/10.3389/fimmu.2024.1390468 (2024).
57. Siegel, C. et al. Complement factor H-related proteins CFHR2 and CFHR5 represent novel ligands for the infection-associated CRASP proteins of *Borrelia burgdorferi*. *PLoS. One* **5**, e13519 (2010).
58. Jumper, J. et al. Highly accurate protein structure prediction with AlphaFold. *Nature* **596**, 583–589 (2021).
59. Tajima, F. Statistical method for testing the neutral mutation hypothesis by DNA polymorphism. *Genetics* **123**, 585–595 (1989).
60. Brangulis, K. et al. Crystal structure of the membrane attack complex assembly inhibitor BGA71 from the Lyme disease agent *Borrelia bavariensis*. *Sci. Rep.* **8**, 1–11 (2018).
61. Teufel, F. et al. SignalP 6.0 predicts all five types of signal peptides using protein language models. *Nat. Biotechnol.* **40**, 1023–1025 (2022).
62. Ohira, M. et al. Lyme neuroborreliosis in Japan: *Borrelia burgdorferi* sensu lato as a cause of meningitis of previously undetermined etiology in hospitalized patients outside of the island of Hokkaido, 2010–2021. *Eur. J. Neurol.* **32**, e70005–e70005 (2025).
63. Margos, G. et al. A new *Borrelia* species defined by multilocus sequence analysis of housekeeping genes. *Appl. Environ. Microbiol.* **75**, 5410–5416 (2009).
64. Stanek, G. et al. Lyme borreliosis: Clinical case definitions for diagnosis and management in Europe. *Clin. Microbiol. Infect.* **17**, 69–79 (2011).

Acknowledgements

Authors gratefully acknowledge the skillful and excellent technical assistance of Martyna Olesiuk. We are greatly indebted to Renate Rutz (University Heidelberg, Germany) for generously providing sheep erythrocytes. We would further like to thank Georg Langebrake and Dr. Kristian Ullrich for their expertise and assistance in relation to bioinformatical analyses.

Author contributions

L.L., designed and performed experiments, analysed the data, and prepared figure 5 and supplementary figure S4. P.K. designed and performed experiments, analysed the data, and prepared figures 4 and 5, and 7, and supplementary figure S3. F.R. designed and performed experiments, analysed the data, and prepared supplementary figure S2. G.M., S.H., V.F. collected samples, isolated *Borrelia* strains and gave conceptual advice. K.S. and H.K. collected and provided *Borrelia* strains. K.B. designed and performed the structural analyses using AlphaFold, and prepared Figs. 2 and 3, and 6, and wrote the main manuscript text. Y.P.L. gave conceptual advice and wrote the main manuscript text. R.E.R. designed and coordinated the research, collected samples, conducted all bioinformatics analyses, analysed data, and prepared figure 1, supplementary figure S1, and supplementary table S1 and S3, and wrote the main manuscript text. P.KR. designed and coordinated the research, gave conceptual advice, prepared figure 8 and supplementary table S2, and wrote the main manuscript text. All authors discussed the results and implications and commented on the manuscript at all stages. All authors reviewed the manuscript.

Funding

Open Access funding enabled and organized by Projekt DEAL.

Declarations

Competing interests

The authors declare no competing interests.

Ethics statement

Collection of blood samples and consent documents were approved by the ethics committee at the University Hospital of Frankfurt (control number 160/10 and 222/14), Goethe University of Frankfurt am Main. All healthy blood donors provided written informed consent in accordance with the Declaration of Helsinki.

Additional information

Supplementary Information The online version contains supplementary material available at https://doi.org/10.1038/s41598-026-43598-2.

Correspondence and requests for materials should be addressed to P.K.

Reprints and permissions information is available at www.nature.com/reprints.

Publisher's note Springer Nature remains neutral with regard to jurisdictional claims in published maps and institutional affiliations.